Li et al. *Zool. Res.* 2023, 44(6): 1080−1094
https://doi.org/10.24272/j.issn.2095-8137.2023.317

ZR | Zoological Research

Article Open Access

Characterization of long-term *ex vivo* expansion of tree shrew spermatogonial stem cells

Cong Li[1,2,3], Rui Bi[2,3], Lin Wang[1,2], Yu-Hua Ma[4], Yong-Gang Yao[2,3,4,5,*], Ping Zheng[1,2,3,4,5,*]

[1] *State Key Laboratory of Genetic Resources and Evolution*, *Kunming Institute of Zoology*, *Chinese Academy of Sciences*, *Kunming*, *Yunnan* 650201, *China*

[2] *Key Laboratory of Animal Models and Human Disease Mechanisms of Yunnan Province*, *Kunming Institute of Zoology*, *Chinese Academy of Sciences*, *Kunming*, *Yunnan* 650201, *China*

[3] *Kunming College of Life Science*, *University of Chinese Academy of Sciences*, *Kunming*, *Yunnan* 650204, *China*

[4] *National Resource Center for Non-Human Primates*, *National Research Facility for Phenotypic & Genetic Analysis of Model Animals (Primate Facility)*, *Kunming Institute of Zoology*, *Chinese Academy of Sciences*, *Kunming*, *Yunnan* 650107, *China*

[5] *KIZ/CUHK Joint Laboratory of Bioresources and Molecular Research in Common Diseases*, *Kunming Institute of Zoology*, *Chinese Academy of Sciences*, *Kunming*, *Yunnan* 650204, *China*

ABSTRACT

Tree shrews (*Tupaia belangeri chinensis*) share a close relationship to primates and have been widely used in biomedical research. We previously established a spermatogonial stem cell (SSC)-based gene editing platform to generate transgenic tree shrews. However, the influences of long-term expansion on tree shrew SSC spermatogenesis potential remain unclear. Here, we examined the *in vivo* spermatogenesis potential of tree shrew SSCs cultured across different passages. We found that SSCs lost spermatogenesis ability after long-term expansion (>50 passages), as indicated by the failure to colonize the seminiferous epithelium and generate donor spermatogonia (SPG)-derived spermatocytes or spermatids marking spermatogenesis. RNA sequencing (RNA-seq) analysis of undifferentiated SPGs across different passages revealed significant gene expression changes after sub-culturing primary SPG lines for more than 40 passages on feeder layers. Specifically, DNA damage response and repair genes (e.g., *MRE11*, *SMC3*, *BLM*, and *GEN1*) were down-regulated, whereas genes associated with mitochondrial function (e.g., *NDUFA9*, *NDUFA8*, *NDUFA13*, and *NDUFB8*) were up-regulated after expansion. The DNA damage accumulation and mitochondrial dysfunction were experimentally validated in high-passage cells. Supplementation with nicotinamide adenine dinucleotide (NAD^+) precursor nicotinamide riboside (NR) exhibited beneficial effects by reducing DNA damage accumulation and mitochondrial dysfunction in SPG elicited by long-term culture. Our research presents a comprehensive analysis of the genetic and physiological attributes critical for the sustained expansion of undifferentiated SSCs in tree shrews and proposes an effective strategy for extended *in vitro* maintenance.

Keywords: Tree shrews; Spermatogonial stem cells; Nicotinamide riboside; DNA damage; Mitochondrial dysfunction

INTRODUCTION

Spermatogenesis relies on spermatogonial stem cells (SSCs), which undergo self-renewal and differentiation to produce gametes throughout the male reproductive lifespan (Kanatsu-Shinohara & Shinohara, 2013; Kubota & Brinster, 2018). Because SSCs can transmit genetic information to the next generation, they are valuable in preserving fertility and generating transgenic animals. Successful long-term *in vitro* expansion of SSCs and SSC-based transgenesis has been reported in mice (Kanatsu-Shinohara et al., 2003), bovine (Izadyar et al., 2002), pigs (Sun et al., 2019; Zheng et al., 2020), and tree shrews (Li et al., 2017). Although expansion of stem cells is necessary for their application, long-term *in vitro* culture can induce genetic and epigenetic changes and impair stem cell properties and function. For instance, human pluripotent stem cells generally acquire recurrent genetic and epigenetic changes during *in vitro* culture, which can compromise stem cell behavior and application (Andrews et al., 2022). Mouse SSCs also display a decline in

Received: 30 September 2023; Accepted: 30 October 2023; Online: 31 October 2023

Foundation items: This work was supported by the Ministry of Science and Technology of China (2021YFF0702700, STI2030-Major Project 2021ZD0200900), National Natural Science Foundation of China (U2102202, U1702284), and Yunnan Province (202305AH340006)

*Corresponding authors, E-mail: yaoyg@mail.kiz.ac.cn; zhengp@mail.kiz.ac.cn

spermatogenesis potential following 5–6 months of expansion in culture (Helsel et al., 2017; Kanatsu-Shinohara et al., 2011; Schmidt et al., 2011). Moreover, cultured undifferentiated spermatogonia (SPG) constitute a heterogeneous population that includes SSCs, progenitor cells, and differentiating SPG (Kanatsu-Shinohara & Shinohara, 2013). Therefore, to facilitate the practical application of SSCs, assessment of the influences of long-term culture on their properties and functions is imperative.

Tree shrews are genetically and evolutionarily close to primates (Fan et al., 2013, 2019; Ye et al., 2021). They are noted for their small body size, rapid reproductive cycle, and short lifespan compared to non-human primates (Yao, 2017), making them advantageous over rodents as models for studying viral infection (Yu et al., 2016; Xu et al., 2020a, 2020b), mycobacterium tuberculosis infection (Zhan et al., 2014), visual system (Familtsev et al., 2016; Lee et al., 2016), and neural system (Savier et al., 2021; Veit et al., 2011; Xiao et al., 2017; Yao, 2017). Intriguingly, recent research also indicated that tree shrews are a good animal model for understanding the functions of primate-specific genes in human spermatogenesis (Liu et al., 2023). Thus, due to their numerous advantages over rodents, tree shrews are considered as a promising animal model for biomedical research and drug screening and testing. Our laboratory has also successfully established a tree shrew gene-editing platform based on the *in vitro* expansion and transplantation of SSCs (Li et al., 2017).

Precise gene editing of SSCs generally requires the clonal growth and expansion of single SSCs (Sun et al., 2019; Zheng et al., 2017). In mice, the number of cultured SSCs doubles approximately every 5.6 days (Kubota et al., 2004), while in tree shrews, a similar doubling takes more than 7 days (Li et al., 2017). Thus, extensive expansion is needed to obtain sufficient cells for transplantation. In this study, we evaluated the impact of long-term expansion on tree shrew SSC functions and molecular changes. In brief, we investigated the properties of tree shrew SPGs sub-cultured over more than 50 passages and found that they lost the ability to colonize seminiferous tubules and undergo spermatogenesis after transplantation into recipient testes. The gene expression signatures associated with DNA damage and mitochondrial defects were identified through RNA sequencing (RNA-seq) and subsequently confirmed through experimental validation. Based on these gene expression changes, we evaluated the efficacy of nicotinamide adenine dinucleotide (NAD^+) precursor nicotinamide riboside (NR) supplementation in preserving tree shrew SSCs during long-term expansion, noting a beneficial effect. Therefore, late-passage tree shrew progenitor-like SPGs offer a bioassay for investigating NR-stimulated signaling pathways, with potential implications for the extended preservation and maintenance of undifferentiated wild-type SPGs *in vitro*.

MATERIALS AND METHODS

Animal use and care

Tree shrews (*Tupaia belangeri chinensis*) (8–18 months old) were obtained from the Experimental Animal Core Facility at the Kunming Institute of Zoology, Chinese Academy of Sciences (Yunnan, China). All experimental procedures and animal care were performed according to the protocols approved by the Institutional Animal Care and Use Committee of the Kunming Institute of Zoology, Chinese Academy of Sciences (IACUC18027).

Preparation of feeder cells

Feeder cells were prepared using the same protocols as reported in previous research (Li et al., 2017, 2021). Briefly, testicular single-cell suspensions from 8–18-month-old tree shrews were plated on gelatin-coated 100 mm dishes (gelatin, Amresco, 9764-500g, USA; 100 mm dish, NEST, 704001). Cells were cultured in Dulbecco's Modified Eagle Medium (DMEM, Thermo Fisher, 12800017, USA) with 10% fetal bovine serum (FBS, Thermo Fisher, Lot# 2441523P, USA). After overnight incubation at 37 °C in a 5% CO_2 atmosphere in the incubator, the adherent cells were collected and passaged at a 1:3 ratio every 5–7 days. These cells can be cultured for many passages due to spontaneous immortalization. Cells at passages 10–20 were cryopreserved for use as feeder cells. Before co-culture with SPGs, the feeder cells at passages 10–20 were treated with 10 μg/mL mitomycin C (mitomycin C, Sigma, M4287, USA) for 3 h, then plated in 24-well plates at a density of 1×10^5 cells/well.

Culture of undifferentiated SPGs

Undifferentiated tree shrew SPGs were maintained in the same culture medium as we reported previously (Li et al., 2017, 2021). In brief, cells were cultured in StemPro-34 serum-free medium (SFM) supplemented with StemPro supplement (Life Technologies, 10639011, USA) and cytokines, including 40 ng/mL recombinant human glial cell line-derived neurotrophic factor (GDNF, R&D, Lot# VQ3222081, USA), 10 ng/mL human epidermal growth factor (EGF, Life Technologies, PHG0311, USA), 1 000 U mouse leukemia inhibitory factor (LIF, Millipore, ESG1107, USA), 2 ng/mL human basic fibroblast growth factor (bFGF, Millipore, GF003, USA), and other factors containing L-glutamine (Sigma, 56-85-9, USA), β-mercaptoethanol (Sigma, M3148, USA), sodium pyruvate (Gibco, 11360-070, USA), MEM non-essential amino acid solution (Gibco, 11140-050, USA), putrescine (Sigma, V900377, USA), and 10% FBS. From passage 0 (P0) until P4, 10 ng/mL recombinant Wnt3a (R&D, Lot# RSK8920011, USA) was added to the culture medium. Tree shrew SPGs were passaged at a 1:3 ratio every 5–7 days. The cells were maintained at 37 °C in a 5% CO_2 atmosphere and cryopreserved following standard procedures using 10% dimethyl sulfoxide (DMSO, Sigma, SY-SJ311, USA) and 90% FBS. Cell line information for the three SSC lines used in this study is shown in Supplementary Table S1. Upon thawing, cryopreservation medium was rinsed from the spermatogonial pellets by twice washing using standard tree shrew spermatogonial culture medium prior to plating.

Cell cycle phase analysis

Undifferentiated tree shrew SPGs were collected and centrifuged at 200 ×*g* for 5 min at room temperature. The cell pellets were then gently re-suspended in 70% ethanol (DW, 10149, China) for 15 min. DNA was counterstained with 50 μg/mL propidium iodide (Beyotime, ST512, China) for 30 min at 37 °C. Cell cycle phase was analyzed using a high-speed analytical flow cytometer (Becton Dickinson, USA). Data were analyzed using FlowJo VX 7.6.1 software (USA).

Sub-G1 analysis

In apoptotic cells, DNA undergoes degradation, resulting in the partial loss of fragmented DNA during sample preparation for fluorescence-activated cell sorting (FACS). Consequently, DNA content in apoptotic cells is often below the 2n level,

known as the sub-G1 phase (Oancea et al., 2006). Here, undifferentiated tree shrew SPGs were collected and centrifuged at 200 ×*g* for 5 min at room temperature. The resulting cell pellets were then gently re-suspended in 70% ethanol for 15 min. The DNA was counterstained with 50 μg/mL propidium iodide for 30 min at 37 °C. Cells at the sub-G1 phase were analyzed using high-speed analytical flow cytometry. Data were analyzed using FlowJo VX 7.6.1 software.

Cell growth rate analysis

Undifferentiated tree shrew SPGs at P10 (low passage) and P50 (high passage) were used to assess growth rate. The same number of cells was seeded in 24-well plates in each passage, and total cell number of each passage was calculated using a cell counter (Countstar BioTech, China) at 7 days post-plating.

Cell proliferation assay

Undifferentiated tree shrew SPGs were seeded in 1.8 cm^2 culture wells in 24-well plates, with a density of 3.5×10^4–$4\times10^4/cm^2$ at each passage. The cells were then labeled with 50 μmol/L BrdU (Sigma-Aldrich, B5002-100MG, USA) for 12 h, followed by fixation in 4% paraformaldehyde (Sigma-Aldrich, 158127-500G, USA) for 10 min. Cells were permeabilized with 0.1% Triton X-100 (Sigma, Lot# SLBW6818, USA) in phosphate-buffered solution (PBS) for 15 min at room temperature, followed by denaturation in 2 mol/L HCl at room temperature for 30 min. After staining with anti-BrdU primary antibody and Cy3-conjugated secondary antibody, the $BrdU^+$ cells were sorted using high-speed analytical flow cytometry (Becton Dickinson, USA). Data were analyzed using FlowJo VX 7.6.1 software. All antibody information is listed in Supplementary Table S2.

Karyotyping

Undifferentiated tree shrew SPGs were incubated with 0.25 μg/mL Colchicine (Sigma-Aldrich, C3915-500MG, USA) for 4 h at 37 °C in a 5% CO_2 atmosphere in the incubator. Cells were collected and cell pellets were gently resuspended with 0.4% KCL (Sigma, Lot# SLBH5524V, USA)/0.4% sodium citrate (Aladdin, S189183-100g, China) (ratio 1:1) and incubated for 15 min at room temperature, followed by fixation with methanol (DM, 104119, China)/glacial acetic acid (Aladdin, Lot# I1712010, China) (ratio 3:1). Fixed cells were dropped onto microscope slides (CITOTEST, 188105W, China), air dried, and baked at 65 °C overnight. The slides were then stained with Giemsa solution (Life Technologies, 10092013, USA) (PBS/Giemsa=250:1) for 10 min and examined using the Leica TCS SP5 confocal microscope system (Leica Microsystems, Germany). At least 40 metaphase spreads were examined in three independent replicates.

Measurement of mitochondrial DNA copy number and telomere length

Genomic DNA was extracted from cultured undifferentiated SPGs using lysis buffer (10% SDS; 0.5 mol/L EDTA; 1 mol/L Tris-HCl, pH=7) supplied with 120 μg/mL proteinase K (BBI, B600169-0002, UK). Telomere length was analyzed based on previous research (Lau et al., 2013). Briefly, primers for telomeres were synthesized (Lau et al., 2013) and telomere length was normalized based on the single-copy nuclear gene hemoglobin subunit beta (*HBB*). Mitochondrial DNA (mtDNA) copy number was measured, as described previously (Bi et al., 2022). In brief, the primers for undifferentiated SPG mtDNA were designed based on the entire mtDNA sequence (Xu et al., 2012). MtDNA content was normalized to the single-copy nuclear gene *HBB*. All primers are provided in Supplementary Table S3.

Reverse transcription-quantitative real-time polymerase chain reaction (RT-qPCR)

Total RNA was extracted from cultured undifferentiated SPGs using TRNzol (Tiangen, Lot# Y1222, Germany). Reverse transcription was performed using a PrimeScript™ RT Reagent Kit with gDNA Eraser (TaKaRa, Lot# AM81755A, Japan). A TB Green™ Premix Ex Taq™ II Kit (Takara, RR820A, Japan) and CFX96TM Real-Time System (Bio-Rad, CFX96Touch, USA) were used for RT-qPCR analysis. The relative mRNA levels of the *FMR1*, *CDK17*, *SMC5*, *FANCM*, *ATP5MG*, *NDUFA8*, *NAMPT*, *LIN28A*, *STRA8*, *SOHLH1*, *FGFR3*, *ETV5*, *DDX4*, *DAZL*, *MSL3*, *ID4*, *MORC1*, *ZBTB43*, *ID3*, *NANOS3*, and *DMRTB1* genes in cultured undifferentiated SPGs were quantified at different passages. Relative mRNA expression levels were normalized by *GAPDH*. All primers for RT-qPCR are provided in Supplementary Table S3.

Immunoblotting

Undifferentiated tree shrew SPGs were collected and lysed in RIPA buffer (Beyotime, P0013J, China) supplemented with proteinase inhibitor (Beyotime, P1006, China). The protein lysate was electrophoresed in 10%–12% sodium dodecyl-sulfate polyacrylamide gel electrophoresis (SDS-PAGE) gels and transferred to polyvinylidene fluoride (PVDF) membranes (Roche, 03010040001, Switzerland). After blocking with 5% skim milk (Biofroxx, Lot# EZ6789B145, Germany), the membranes were incubated with primary antibodies (Supplementary Table S2) at 4 °C overnight. After three washes with 1×Tris-buffered saline with Tween 20 (TBST) (each 5 min), the membranes were incubated with the corresponding horseradish peroxidase (HRP)-conjugated secondary antibodies for 1 h at room temperature. After thrice washing with 1×TBST buffer (each 5 min), the bands were detected using enhanced chemiluminescence (ECL) reagent (Beyotime, P0018FS, China) from the ProteinSimple FluorChem system (protein simple, FluorChem M FM0561, USA).

Undifferentiated SPG transplantation

Recipient tree shrew preparation and cell transplantation were performed following previous research (Bi et al., 2021a, b; Li et al., 2017). In total, 15 one-year-old tree shrews were used as recipients. Briefly, undifferentiated SPGs were infected with lentiviral simian immunodeficiency virus (SIV) expressing GAE-CAG-EGFP/WPRE (SIV-EGFP). The EGFP-expressing cells were collected using FACS. The enriched $EGFP^+$ cells were further cultured and the expression of EGFP proteins was validated by immunoblot analysis. For transplantation, the EGFP-expressing cells (5×10^5–6×10^5) were mixed with methylene blue (Macklin, Lot# C11748711, China), and transplanted into the recipient seminiferous tubules of the testes through the efferent ducts. Transplantation efficiency was monitored using methylene blue. The cells (3×10^5–4×10^5) were transplanted into the recipient testes. In total, three tree shrew SSC lines were used to assess spermatogenic capacity.

Immunofluorescence staining

The recipient testes were collected and fixed in 4%

paraformaldehyde. After sequential dehydration with 15% and 30% sucrose (Lot# I425BA0004, China), the testes were embedded in optimal cutting temperature compound (OCT, 4583, USA), sliced into 10 μm sections, and stored at –80 °C. Slides were randomly picked for immunofluorescence staining using standard procedures. In brief, the testicular sections were washed three times in PBS for 30 min, followed by permeabilization with 0.25% Triton X-100 for 15 min at room temperature. For cell immunofluorescence staining, the cultured cells were fixed in 4% paraformaldehyde for 15 min and permeabilized with 0.2% Triton X-100 in PBS for 15 min at room temperature. The cells and sections were then blocked with 5% bovine serum albumin (BSA, Macklin, B824162-10g, China) for 1 h at room temperature and stained with primary antibodies diluted in 1% BSA at 4 °C overnight. The cells and sections were washed three times with PBS and stained with Alexa Fluor-conjugated secondary antibodies for 1 h at room temperature. The nuclei were then counterstained with 4',6-diamidino-2-phenylindole (DAPI, Sigma-Aldrich, D9542-5MG, USA). The cells and sections were sealed with 80% glycerin (Solarbio, G8190, China) and photographed using confocal laser microscopy (FV1000, Japan) or high-resolution fluorescence microscopy (LSM880, Germany). All antibody information is provided in Supplementary Table S2.

TUNEL staining

TUNEL staining was performed on the undifferentiated tree shrew SPGs using a TUNEL FITC Apoptosis Detection Kit (Vazyme, A111-02, China) according to the manufacturer's instructions. Samples treated with DNase I were included as positive controls.

RNA-seq library preparation, sequencing, and data analyses

Total RNA was extracted from undifferentiated tree shrew SPGs using TRNzol. Two independent biological samples were prepared. RNA-seq was performed on the Illumina NovaSeq 6000 system (USA). Clean sequence reads were mapped to the tree shrew reference genome (KIZ v3) (Ye et al., 2021) using TopHat2 software and coding gene expression was calculated using Cufflinks (Trapnell et al., 2012). Cuffdiff software (Trapnell et al., 2013) was used to determine differentially expressed genes (DEGs). Gene Ontology (GO) enrichment analysis was performed using online tools (http://geneontology.org/). Heatmaps were draw using the "gplot" package in R. The RNA-seq data were deposited in the Gene Expression Omnibus (GEO) database (GSE228744).

Measurement of reactive oxygen species (ROS)

Total ROS levels were detected in undifferentiated tree shrew SPGs using a Reactive Oxygen Species Assay Kit (Beyotime, S0033S, China), which predominantly detects hydrogen peroxide content. In brief, undifferentiated SPGs were collected and stained with 1 μmol/L or 10 μmol/L 2',7'-dichlorodihydrofluorescein diacetate (DCFH-DA) for 20 min at 37 °C. Analysis was performed by high-speed analytical flow cytometry (Becton Dickinson, USA). Data were analyzed using FlowJo VX 7.6.1 software.

Adenosine triphosphate (ATP) measurement and NAD^+ quantification

Low- and high-passage undifferentiated tree shrew SPGs with or without NR treatment were used to measure ATP levels and NAD^+ concentration. Cell pellets were harvested for measurement. An Enhanced ATP Assay Kit (Beyotime, Lot# 081621220214, China) was used to detect ATP levels according to the manufacturer's instructions. Briefly, cell pellets were processed using lysates, followed by centrifugation at 12 000 ×*g* for 5 min at 4 °C. The resulting supernatant was used for ATP detection. An NAD^+/NADH Assay Kit (Beyotime, Lot# 112222230403, China) was used to quantify NAD^+ concentration according to the manufacturer's instructions. In brief, cell pellets were processed using NAD^+/NADH extraction solution, followed by centrifugation at 12 000 ×*g* for 10 min at 4 °C to obtain the supernatant for NAD^+ detection.

Sperm genotyping

We measured EGFP expression in spermatozoa from transplanted individuals to detect insertion of the EGFP fragment in the genome. Briefly, genomic DNA from spermatozoa was extracted using lysis buffer (10% SDS; 0.5 mol/L EDTA; 1 mol/L Tris-HCl, pH=7) with proteinase K. PCR amplification of the EGFP fragment was performed using the following cycle conditions (95 °C for 3 min, 30 cycles at 95 °C for 30 s, 60 °C for 30 s, and 72 °C for 30 s, with a final 10 min elongation at 72 °C) and indicated primer pairs (Supplementary Table S3).

Alkaline comet assay

The alkaline comet assay was performed as described in previous studies (Swain & Rao, 2011; Zhao et al., 2015, 2018). In brief, glass slides were coated with 0.8% agarose (BBI, A600015-0025, UK) for 5 s and air dried. A single-cell suspension (10^3 cells/μL) was mixed with 70 μL of 0.8% low-melting-point agarose maintained at 37 °C. The cell-agarose suspension was spread onto the previous slides and covered with a coverslip. After sitting at 4 °C for 10 min, the slides were incubated in lysis solution (2.5 mol/L NaCl, 100 mmol/L Na_2EDTA, 10 mmol/L Tris, 1% N-lauroylsarcosine, 1% TritonX-100, pH=10.0) for 1 h at 4 °C in the dark without a coverslip, then washed with ddH_2O and incubated with cold electrophoresis buffer (1 mmol/L Na_2EDTA; 0.3 mol/L NaOH; pH>13) for 20 min. Electrophoresis was performed for 30 min at 35 V and 300 mA. Slides were washed with ddH_2O and fixed in ethanol until air dried. After counterstaining with DAPI (10 ng/mL), cells were immediately analyzed. Comets were analyzed using Komet 7 Comet Assay software (Andor Technology, USA). The olive moment, which quantifies both the amount and distribution of DNA in the tail, was determined. At least 200 cells were analyzed across three independent experiments.

Alkaline phosphatase (AP) staining

The activity of AP was analyzed using an Alkaline Phosphatase Assay Kit (Beyotime, P0321S, China) according to the manufacturer's instructions. Briefly, undifferentiated tree shrew SPGs at different passages (P23, P44, and P62) were fixed in 4% paraformaldehyde for 15 min, then counterstained with working solution (Beyotime, P0321S, China) for 30 min at 37 °C. The cells were photographed using an optical microscope.

Statistical analysis

All data were analyzed with GraphPad Prism v8 (GraphPad Software, USA) using two-tailed Student's *t*-test. A *P*-value of less than 0.05 was considered statistically significant. All data were provided as means±standard deviation (*SD*).

RESULTS

Long-term expansion of undifferentiated SPGs decreased SSC population and spermatogenesis potential

We first evaluated the influence of long-term expansion on the growth of undifferentiated tree shrew SPGs. The undifferentiated SPGs were expanded in culture medium (Li et al., 2017) over one year (>85 passages). The cell culture passages were classified as low (<30 passages), medium (30–50 passages), and high groups (>50 passages). High-passage SPG colonies displayed similar morphology as low-passage colonies (Figure 1A). Flow cytometry showed that long-term expansion (>50 passages) did not affect basic cell cycle properties (Figure 1B). Moreover, cell proliferation rates evaluated using the BrdU incorporation assay (Figure 1C), as well as growth rate curves (Figure 1D), were not altered by *in vitro* expansion. TUNEL staining (Figure 1E) and sub-G1 stage analysis (Oancea et al., 2006) (Figure 1F) revealed that extended culture had no significant influence on apoptosis.

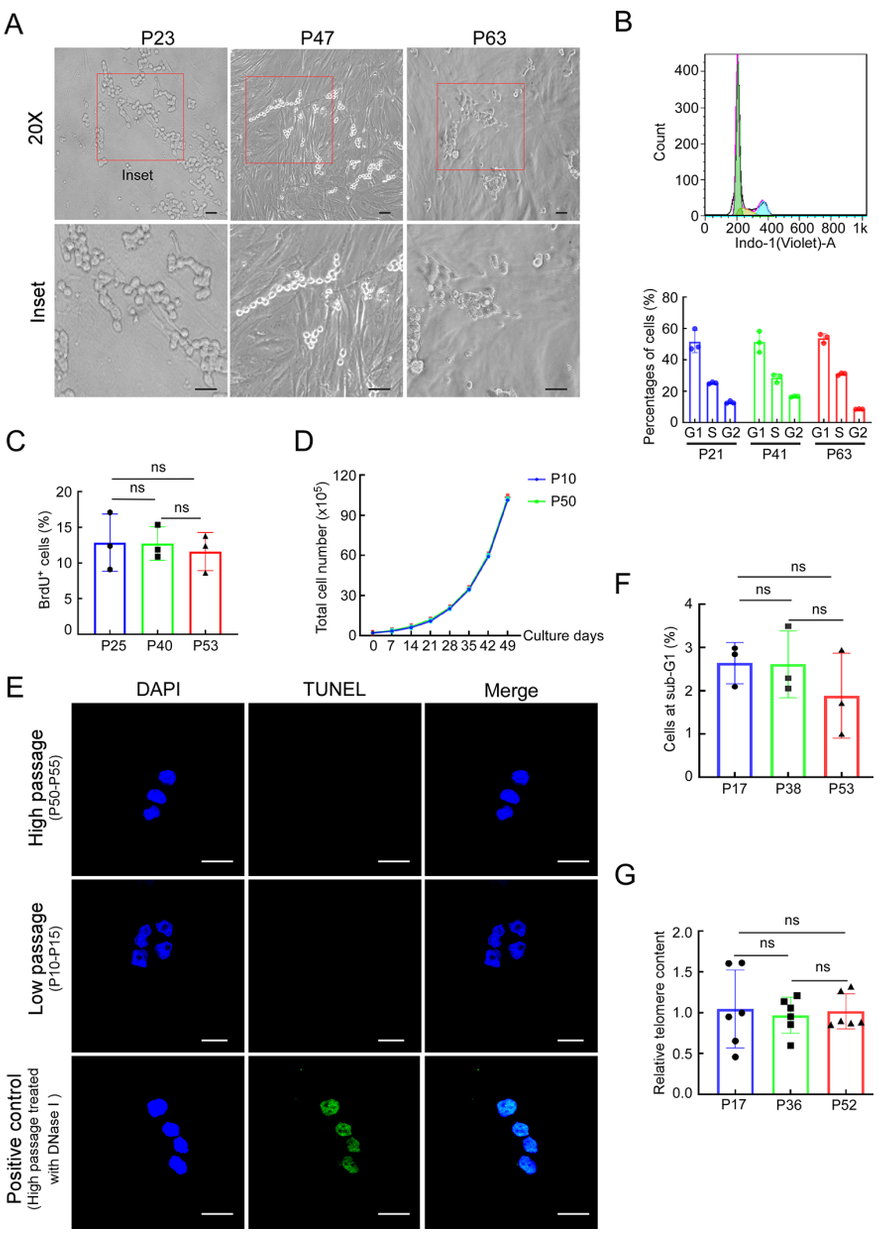

Figure 1 Long-term expansion did not affect basic properties of undifferentiated tree shrew SPGs

A: Representative bright field images of cultured undifferentiated tree shrew SPGs at different passages (P23, P47, and P63). Insets showed higher magnification of undifferentiated tree shrew SPGs indicated in red squares. Scale bars: 20 μm. B: Cell cycle distribution was analyzed by flow cytometry. Upper panel shows flow cytometry profile. Lower panel shows distribution of cell cycle phase at different passages (P21, P41, and P63) across three independent replicates. C: Proliferative cells were labeled by BrdU. FACS analysis revealed that undifferentiated tree shrew SPGs at different passages (P25, P40, and P53) had similar proliferation rates in three independent replications. D: Growth curve of undifferentiated tree shrew SPGs at different passages (P10 and P50). E: TUNEL staining did not detect positive cells in low-passage (P10–P15) and high-passage (P50–P55) undifferentiated SPGs. Scale bars: 20 μm. F: Sub-G1 distribution was analyzed by flow cytometry at different passages (P17, P38, and P53) across three independent replicates. G: Telomeric DNA content was determined in undifferentiated tree shrew SPGs at different passages (P17, P36, and P52). All SPGs at different passages showed comparable telomeric DNA content across three independent replicates. Data are mean±standard deviation (*SD*). ns: Not significant; two-tailed Student's *t*-test.

Continuous cell division can induce telomere attrition in cultured cells (Rubin, 2002). Thus, we measured telomere length by qPCR examination of telomeric DNA (Lau et al., 2013), and found no induction of telomere attrition during long-term expansion (Figure 1G). Taken together, these results suggest that long-term expansion (>50 passages) does not affect the basic properties of undifferentiated tree shrew SPGs.

We next examined whether long-term expansion could reduce the SSC population in undifferentiated SPGs. Previous studies have shown that AP is active in undifferentiated mouse SPGs (Kubota et al., 2004). Similarly, undifferentiated tree shrew SPGs were positive for AP, and long-term culture did not compromise AP activity (Figure 2A). Consistently,

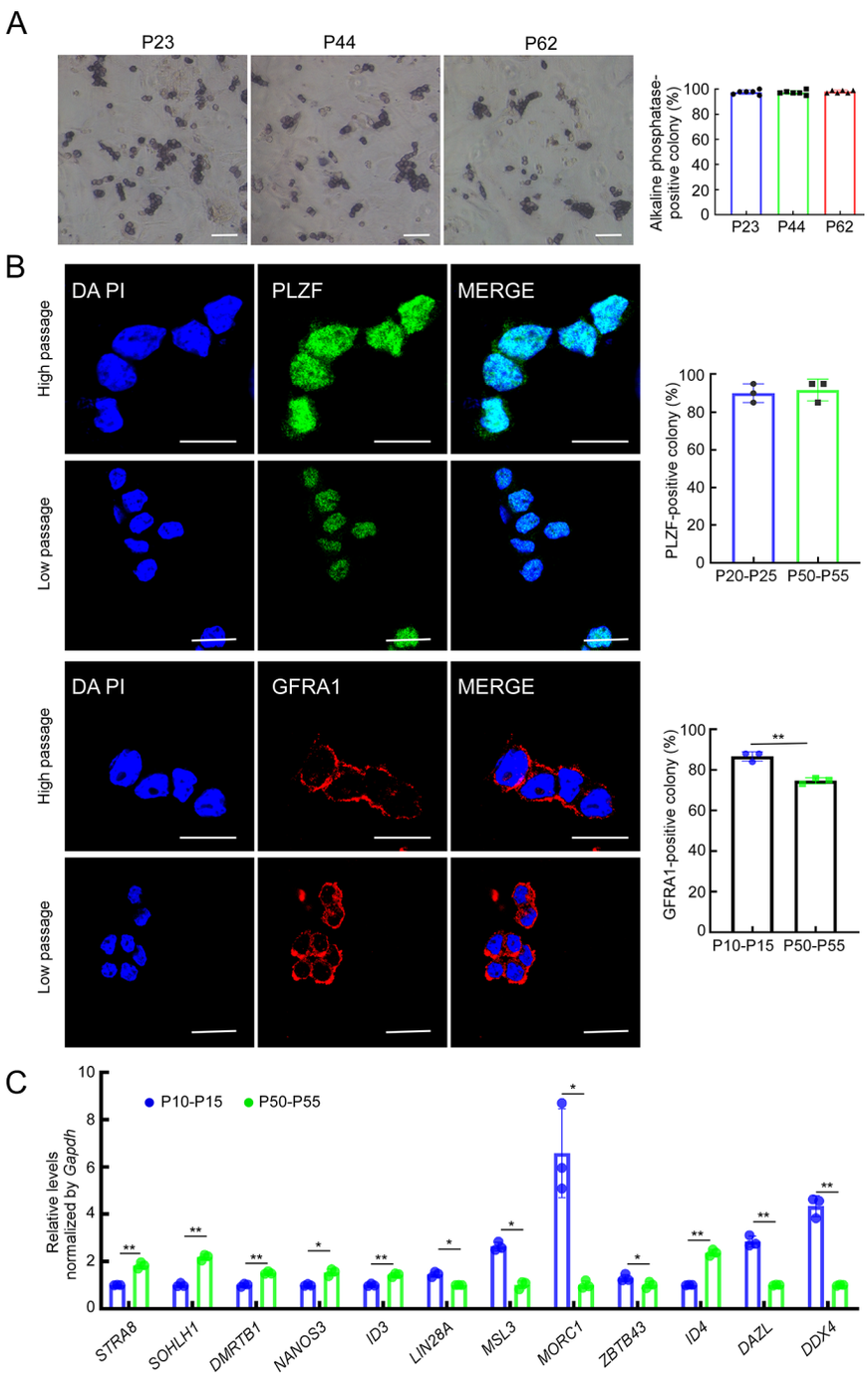

Figure 2 Long-term expansion of undifferentiated tree shrew SPGs led to a decrease in authentic SSC population

A: Long-term cultured undifferentiated tree shrew SPGs retained alkaline phosphatase (AP) activity. Left panel shows representative images of AP staining in SPGs at P23, P44, and P62, respectively, and right panel shows quantification. At least 100 colonies were calculated in six independent experiments. Scale bars: 50 μm. B: Immunofluorescence staining of PLZF and GFRA1. Left panel shows representative images, and right panel shows quantification. Twenty undifferentiated SPG colonies were analyzed in each group across three independent replicates. Scale bars: 20 μm. We grouped SPGs at close passages as one group. For instance, P20–25 means SPGs at passages 20 to 25. C: RT-qPCR validation of mRNA expression of marker genes from three independent replicates. Data are mean±standard deviation (*SD*). *: $P<0.05$; **: $P<0.01$; two-tailed Student's *t*-test.

immunofluorescence staining showed that PLZF, a broad marker of undifferentiated SPGs (Zheng et al., 2017), was normally expressed in the high-passage SPGs (Figure 2B). We further examined GFRA1, a marker of type A undifferentiated SPGs (potential SSCs) in mice (Shami et al., 2020). Results showed that GFRA1 expression was significantly decreased in the high-passage colonies compared to the low-passage cell colonies (Figure 2B), suggesting that long-term expansion may reduce the SSC population in culture. We also examined various markers of undifferentiated SPGs (*MSL3*, *MORC1*, *LIN28A*, *ZBTB43*, and *ID4*), differentiated SPGs (*STRA8*, *SOHLH1*, *DMRTB1*, *NANOS3*, and *ID3*) and germ cells (*DAZL* and *DDX4*) based on RT-qPCR (Figure 2C). The expression of all differentiated SPG markers was increased in high passage cells. Intriguingly, undifferentiated SPG markers exhibited distinct change patterns. *LIN28A*, *MSL3*, *ZBTB43* and *MORC1*, which are highly expressed in early state undifferentiated SPGs (Shami et al., 2020), showed a decrease in high passage cells. Conversely, the transcription of *ID4,* which is highly expressed in late-stage undifferentiated SPGs in humans and mice (Shami et al., 2020), was increased in the high-passage cells. The expression levels of *DAZL* and *DDX4*, known to decline with germ cell development (Chen et al., 2018; Han et al., 2018), were decreased in high-passage SPGs, indicating a reduction in the number of undifferentiated SPGs. Taken together, these findings suggest that long-term expansion may decrease the SSC population in culture.

Long-term expansion of undifferentiated SPGs compromised *in vivo* spermatogenesis potential after transplantation

Donor germline-derived spermatogenesis provides a way in which to track the relative abundance of functional SSCs in testicular cell cultures (Nagano et al., 1998). To examine whether long-term tree shrew cultured SSCs retain spermatogenesis potential, we performed a transplantation assay following previous studies (Brinster & Zimmermann, 1994; Li et al., 2017). SPGs at different passages were infected with lentiviral SIV-EGFP and EGFP expression was validated by immunoblot and FACS analyses (Figure 3A, B). EGFP-expressing cells enriched via flow cytometry were propagated for several passages before transplantation. Cells (3×10^5–4×10^5) were transplanted into recipient testes and transplantation efficiency was monitored by methylene blue mixed with the cell suspension (Figure 3C). At 2–3 months following transplantation, spermatogenesis was evaluated by the presence of EGFP-positive germ cells. Under a fluorescent dissection microscope, green seminiferous tubules were clearly visible in most recipient testes transplanted with undifferentiated SPGs at P22 (six out of eight testes), whereas no green seminiferous tubules were visible in testes transplanted with SPGs at P55 (zero out of 10 testes) or P80 (zero out of two testes) for all three cell lines (Figure 3D). Immunofluorescence staining of testicular tissue sections further confirmed the presence of EGFP-expressing germ cells at different developmental stages in recipient testes transplanted with low-passage (P22) SPGs (Figure 3E). However, no green cells were detected in the seminiferous tubules of recipient testes receiving high-passage cell transplantation (P55 or P80) (Figure 3E). Moreover, spermatozoa harvested from the epididymis were examined using PCR, verifying genomic insertion of the EGFP fragment in spermatozoa generated from transplanted SPGs at P22 (Figure 3F). Collectively, these results suggest that high-passage expansion of undifferentiated tree shrew SPGs (>50 passages) impairs stem cell identity and spermatogenesis potential.

RNA-seq analysis revealed significant changes in gene expression profiles after long-term undifferentiated SPG culture

To investigate changes in gene expression associated with loss of spermatogenesis potential after long-term expansion of SSCs, we performed RNA-seq analysis of tree shrew SPGs expanded for various passages (17, 26, 41, and 53 passages). Hierarchical clustering revealed that cells at P17 and P26 clustered together, whereas cells at P41 and P53 clustered together (Figure 4A). These results suggest that SPGs at P41 share similarities with those at P53, indicating loss of spermatogenesis potential. To examine alterations in gene expression during the culture process, we analyzed DEGs across the four distinct passages. In total, 3 932 DEGs that met the established criteria (P<0.05, q<0.05, and fold-change≥2) were identified (Supplementary Dataset S1). Notably, genes highly expressed in primitive mouse, monkey, or human SSCs (e.g., *LIN28A*, *MORC1*, *ZBTB43*, *GFRA1*, *FMR1*, *PIIWIL4*, and *CDK17*) were down-regulated during prolonged culture. Conversely, genes indicative of differentiating SPGs (e.g., *SOHLH1*, *STRA8*, *DMRT1*, and *DMRTB1*) were up-regulated (Guo et al., 2018; Shami et al., 2020) (Figure 4B). These changes in gene expression are consistent with the SPG transplantation results. Intriguingly, most DEGs (3 418/3 932, 86.93%) were grouped into two clusters: one showing up-regulation and one showing down-regulation in higher-passage cells (P41 and P53) (Figure 4C; Supplementary Dataset S1). GO enrichment analysis revealed that down-regulated genes in higher passage cells were enriched in DNA repair, cell migration, homologous recombination (HR)-mediated DNA double strand break (DSB) repair, stem cell maintenance, germ cell development, and spermatogenesis, while up-regulated genes in higher passage cells were enriched in aerobic respiration, mitochondrial ATP synthesis-coupled proton transport, oxidative respiratory chain, response to oxidative stress, cell redox homeostasis, and aging (Figure 4C; Supplementary Dataset S1). The changes in expression of genes related to undifferentiated SSCs (e.g., *FMR1* and *CDK17*), DNA repair (e.g., *SMC5* and *FANCM*), and mitochondrial ATP synthesis-coupled proton transport (e.g., *ATP5MG* and *NDUFA8*) were corroborated by RT-qPCR (Figure 4D). Taken together, these observations suggest that long-term culture may cause DNA damage accumulation and mitochondrial functional alterations, which are relevant to the loss of stem cell function (Helsel et al., 2017).

Long-term culture increased DNA damage and altered mitochondria metabolism in undifferentiated tree shrew SPGs

Prolonged *in vitro* expansion of stem cells has been associated with the accumulation of DNA damage and genetic alterations, factors that may precipitate stem cell apoptosis or compromise stem cell functionality (Yamanaka, 2020; Zheng, 2022). To corroborate the presence of DNA damage in long-term cultured SPGs, we conducted gene expression analyses. Notably, both immunoblot assays (Figure 5A; Supplementary Figure S1A) and immunofluorescence staining (Figure 5B) revealed that levels of γH2AX, a marker of DNA DSBs

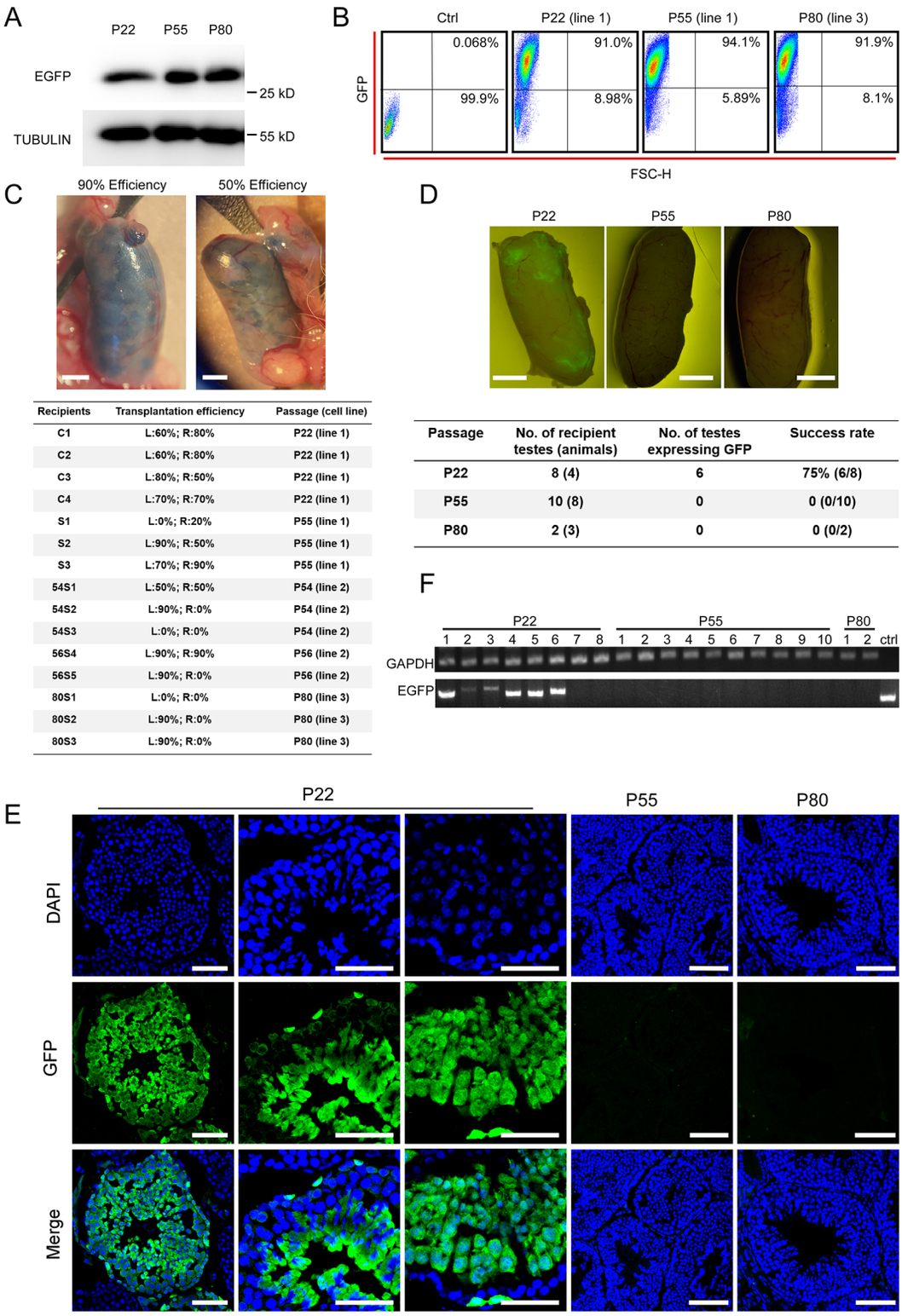

Recipients	Transplantation efficiency	Passage (cell line)
C1	L:60%; R:80%	P22 (line 1)
C2	L:60%; R:80%	P22 (line 1)
C3	L:80%; R:50%	P22 (line 1)
C4	L:70%; R:70%	P22 (line 1)
S1	L:0%; R:20%	P55 (line 1)
S2	L:90%; R:50%	P55 (line 1)
S3	L:70%; R:90%	P55 (line 1)
54S1	L:50%; R:50%	P54 (line 2)
54S2	L:90%; R:0%	P54 (line 2)
54S3	L:0%; R:0%	P54 (line 2)
56S4	L:90%; R:90%	P56 (line 2)
56S5	L:90%; R:0%	P56 (line 2)
80S1	L:0%; R:0%	P80 (line 3)
80S2	L:90%; R:0%	P80 (line 3)
80S3	L:90%; R:0%	P80 (line 3)

Passage	No. of recipient testes (animals)	No. of testes expressing GFP	Success rate
P22	8 (4)	6	75% (6/8)
P55	10 (8)	0	0 (0/10)
P80	2 (3)	0	0 (0/2)

Figure 3 Long-term expansion of undifferentiated tree shrew SPGs impaired *in vivo* spermatogenesis potential after transplantation

A: Immunoblotting confirmed expression of EGFP in undifferentiated SPGs infected with lentiviral SIV-EGFP. B: EGFP$^+$ cells were sorted and enriched by flow cytometry. Control (Ctrl), wild-type undifferentiated tree shrew SPGs. C: SPG transplantation information. Upper panel shows representative images of SPG transplantation into recipient testes with different efficiencies. Transplantation efficiency was monitored by methylene blue, with approximately 3×10^5–4×10^5 cells transplanted into each recipient testis. Lower panel shows summary of transplantation information. L, left testis. R, right testis. Scale bars: 1 mm. D: After transplantation, undifferentiated SPGs at low passage (P22) but not high passage (P55 and P80) showed spermatogenesis potential. Upper panel shows representative images of recipient testes examined 2–3 months following transplantation. Lower panel shows summary of transplantation results. Scale bars: 2 mm. E: Representative images of immunofluorescence staining of EGFP in testicular sections. Scale bars: 50 μm. F: PCR detection of EGFP fragment inserted in sperm genome. Amplification of *GAPDH* was used as an inner positive control for successful PCR. Control (ctrl), SIV-EGFP vector.

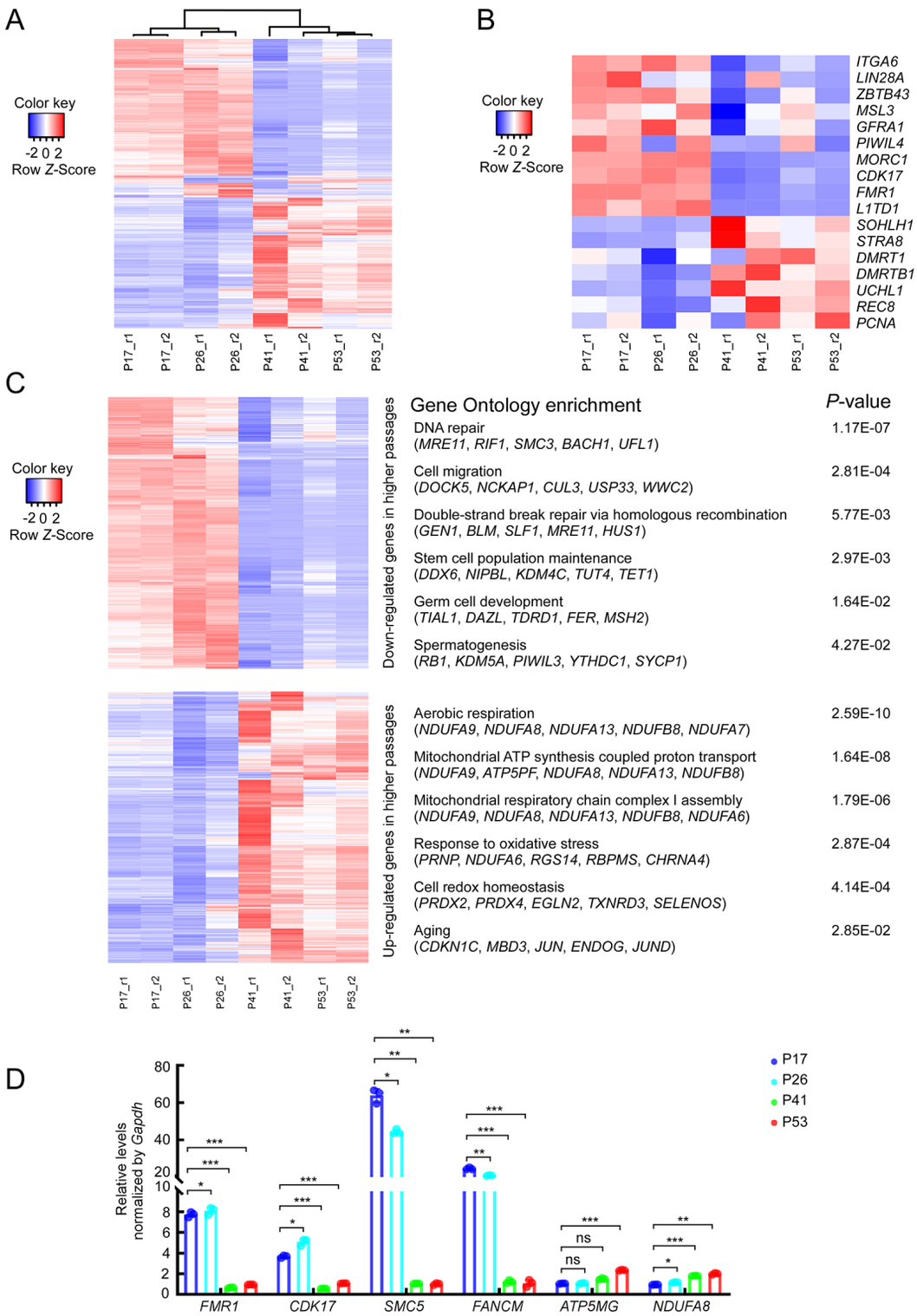

Figure 4 RNA-seq analysis revealed significant gene expression profile changes after long-term culture of undifferentiated tree shrew SPGs

A: Undifferentiated tree shrew SPGs at different passages (P17, P26, P41, and P53) were analyzed by hierarchical clustering. SPGs at each passage consisted of two replicates (marked r1 and r2). B: Expression heatmap of marker genes for undifferentiated and differentiating SPGs. C: Down- and up-regulated DEGs in high-passage cells, with corresponding top GO enriched terms. D: RT-qPCR validation of representative DEGs in cultured undifferentiated SPGs at different passages (P17, P26, P41, and P53). Each passage consisted of three independent biological replicates. Data are mean±standard deviation (*SD*). ns: Not significant; *: $P<0.05$; **: $P<0.01$; ***: $P<0.001$; two-tailed Student's *t*-test.

(Rogakou et al., 1998; Zhang et al., 2023), increased with culture. Alkaline comet assays, which quantify DNA breaks at the single-cell level, further verified the increase in DNA fragmentation (Swain & Rao, 2011; Zhao et al., 2015) (Figure 5C). Despite the induction of DNA breaks, long-term propagation did not heighten the risk of aneuploidy, with more

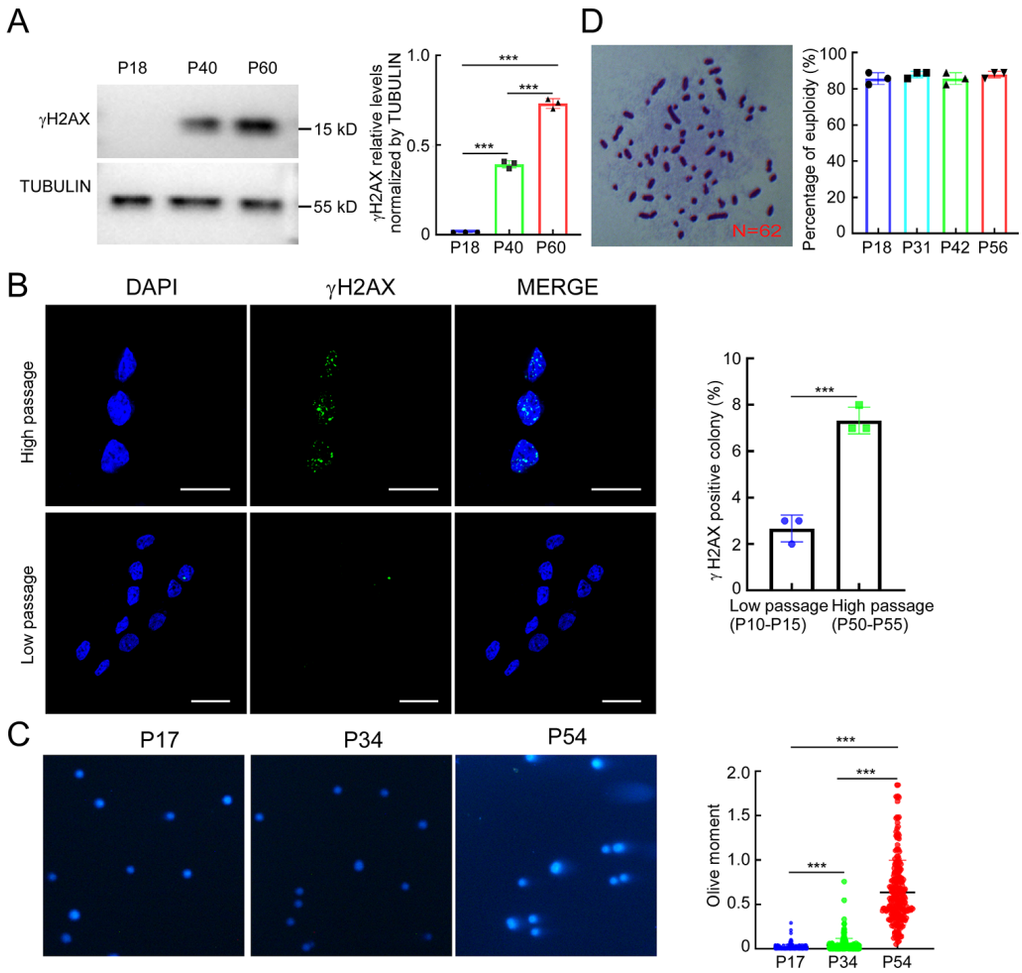

Figure 5 Long-term culture increased DNA damage in undifferentiated tree shrew SPGs

A: Long-term culture of undifferentiated tree shrew SPGs increased γH2AX levels, indicative of greater DNA damage. Right panel shows quantification of band intensity. B: Immunofluorescence staining of γH2AX. Left panel shows representative images, and right panel shows quantification. Cells containing at least five γH2AX-stained foci were considered as positive. Twenty undifferentiated SPG colonies were analyzed in each group across three independent replicates. Scale bars: 20 μm. C: Alkaline comet assay validated the increase in DNA DSBs. Left panel shows representative images of comet tails. Right panel shows quantification of comet tail length. At least 200 tails were analyzed in each group across three independent replicates. D: Undifferentiated tree shrew SPGs maintained a normal karyotype after long-term culture. At least 40 metaphase spreads in three independent replicates were analyzed. Data are mean±standard deviation (*SD*). ***: $P<0.001$; two-tailed Student's *t*-test.

than 80% of high-passage undifferentiated SPGs maintaining a normal karyotype (2*n*=62) (Figure 5D). These observations are consistent with previous research on high-passage mouse SSCs (Kanatsu-Shinohara et al., 2019).

Extended culture led to the up-regulation of various genes associated with mitochondrial ATP synthesis, oxidative phosphorylation, and oxidative stress responses. Thus, we speculated that mitochondria may undergo marked alterations following prolonged culture. Indeed, an increase in mtDNA copy number was observed with culture (Figure 6A), indicative of elevated mitochondrial mass. Immunofluorescence staining of TOM20, a protein located in the mitochondrial outer membrane (Rath et al., 2021), showed that its distribution was not altered in high-passage SPGs, although a slight increase in fluorescence intensity was noted (Figure 6B). In accordance with the increase in mitochondrial mass, elevated ATP synthesis was detected in the high-passage SPGs (Figure 6C). In addition, levels of ROS, which are byproducts of oxidative phosphorylation, were also elevated in high-passage SPGs, as measured by 1 or 10 μmol/L DCFH-DA assays for the detection of hydrogen peroxide (Figure 6D). These data collectively suggest that extended culture of SPGs disrupts mitochondrial homeostasis and alters the metabolic state of stem cells, as reported in previous studies (Chen et al., 2020; Ryall et al., 2015; Wu et al., 2016).

Addition of NR in culture partially alleviated DNA damage and metabolic activity

Our findings indicated that undifferentiated tree shrew SPGs subjected to long-term culture exhibited various phenotypes, including altered mitochondrial homeostasis, increased oxidative stress, and induced DNA damage. DNA damage has been linked to epigenetic modifications and aging phenotypes (Yang et al., 2023), while metabolic status also plays a critical role in determining cell identity (Lord & Nixon, 2020; Voigt et al., 2021; Wang et al., 2022). Therefore, we explored whether DNA damage and oxidative stress can be alleviated in tree shrew SPGs during culture. Oxidized NAD^+ plays an important role in redox reactions and is an essential substrate for various enzymes, including sirtuins (SIRTs) and poly (ADP-ribose) polymerases (PARPs) (Zapata-Pérez et al., 2021). SIRTs are a family of deacetylases essential for regulating energy metabolism and mitochondrial function, whereas

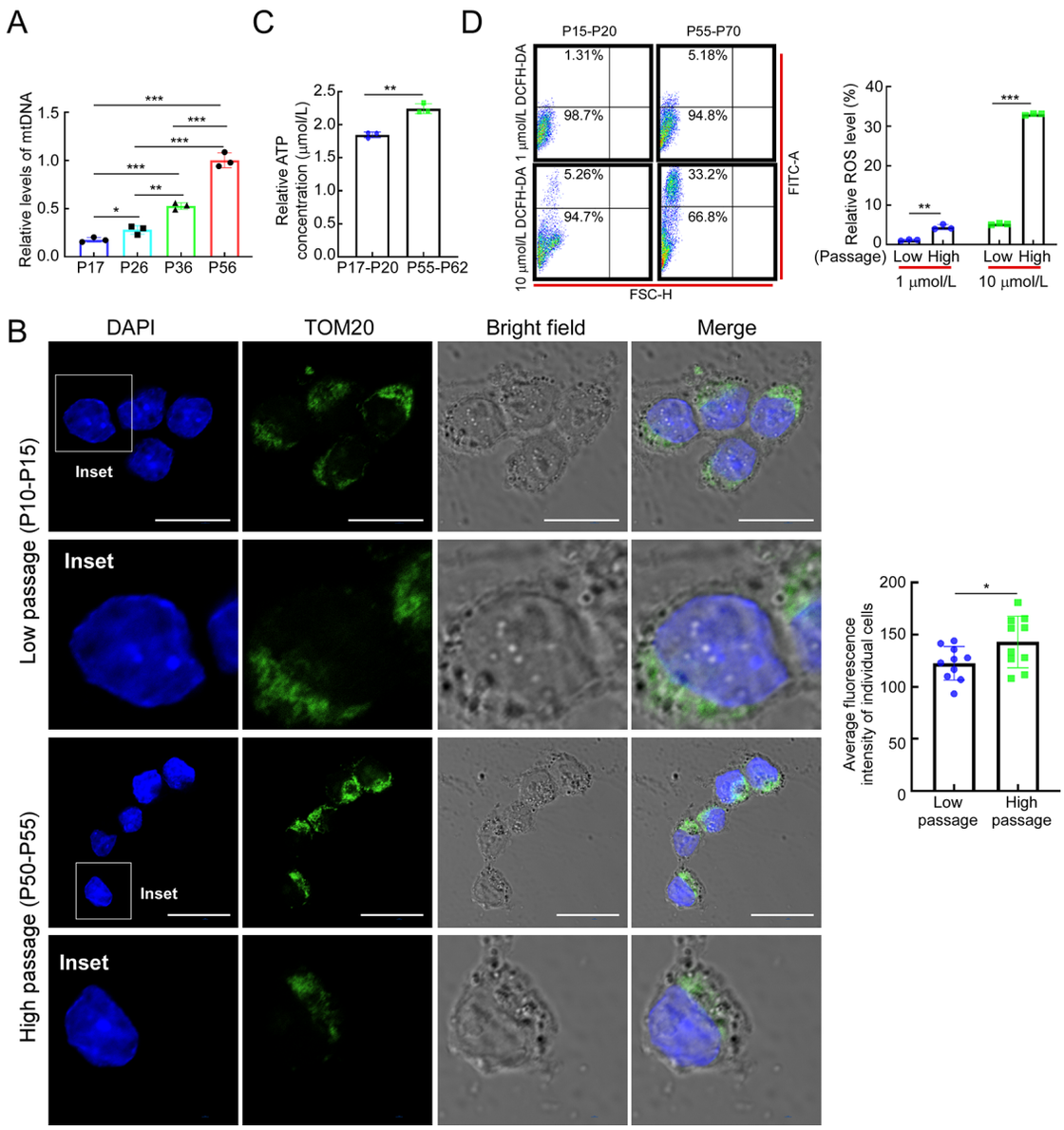

Figure 6 Long-term culture altered mitochondrial metabolism of undifferentiated tree shrew SPGs

A: Mitochondrial DNA copy number was determined in cultured undifferentiated SPGs at P17, P26, P36, and P56. Each passage consisted of three independent replicates. B: Immunofluorescence staining of TOM20. Insets shows higher magnification of undifferentiated tree shrew SPGs indicated in squares. Fluorescence intensity of 10 undifferentiated SPG colonies were analyzed in each group (right panel). Scale bars: 20 μm. C: Cellular ATP concentration increased with culture in three independent replicates. D: Cellular ROS levels were significantly increased in cultured undifferentiated SPGs at high passage (high, P55–P70) relative to those at low passage (low, P15–P20). Cultured SPGs were treated by 1 or 10 μmol/L DCFH-DA and detected using flow cytometry. Each low- and high-passage sample consisted of three independent replicates. Left panel shows representative images of flow cytometry profiles. Right panel shows quantification. Data are mean±standard deviation (*SD*). *: $P<0.05$; **: $P<0.01$; ***: $P<0.001$; ***: $P<0.0001$; two-tailed Student's *t*-test.

PARPs play a role in DNA damage repair (Garten et al., 2015). NAD^+ can be synthesized from its precursors, nicotinamide (NAM) and NR, through the nicotinamide phosphoribosyltransferase (NAMPT) and nicotinamide riboside kinase (NRK) enzymes, respectively (Bieganowski & Brenner, 2004; Mouchiroud et al., 2013). Interestingly, both RNA and protein expression levels of NAMPT, the rate-limiting enzyme for the conversion of NAM to NAD^+ (Garten et al., 2015), were significantly reduced in high-passage SPGs (Figure 7A, B; Supplementary Figure S1B). Based on these observations, we hypothesized that NAD^+ levels may decline with extended culture and that culture medium supplementation with NR may serve as a potential strategy for salvaging NAD^+ and alleviating the adverse effects of long-term culture. Indeed, the concentration of NAD^+ showed a significant decline in high-passage SPGs compared to low-passage cells (Figure 7C).

We next examined the impact of NR inclusion on SPGs. First, we evaluated the dose effect of NR on NAD^+ generation. Undifferentiated SPGs at P53 were cultured with 0, 25, 50, and 100 μmol/L NR for one passage. Results showed that 100 μmol/L NR treatment stimulated the highest level of NAD^+ generation (Figure 7D). Thus, 100 μmol/L NR was used for downstream experiments. Undifferentiated SPGs at P44 were treated with 100 μmol/L NR for one and three passages, respectively. Results showed that continuous treatment

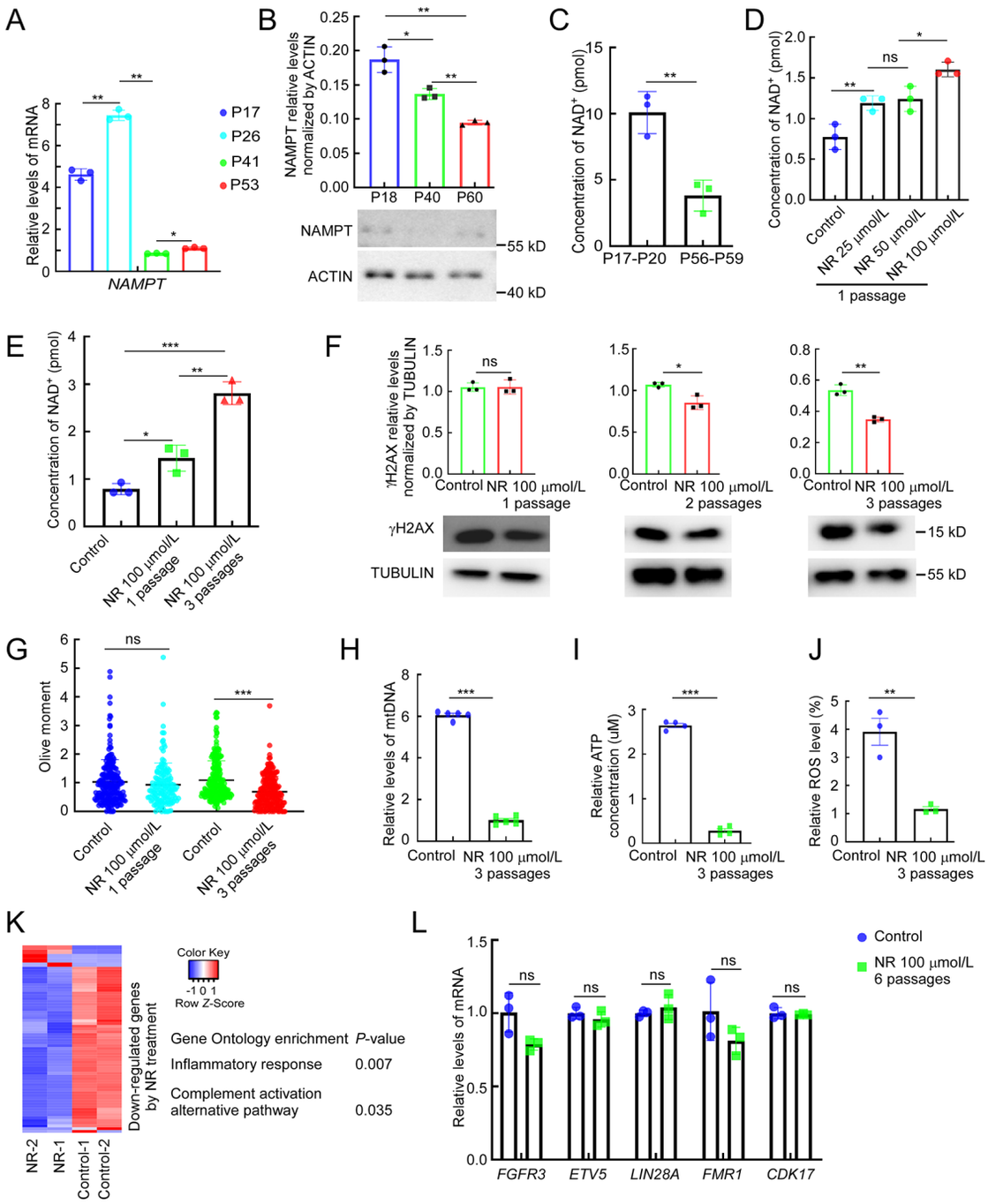

Figure 7 Inclusion of NR in culture medium partially alleviated DNA damage and metabolic impairments

A: Relative mRNA levels of *NAMPT* in undifferentiated tree shrew SPGs cultured for different passages (P17, P26, P41, and P53). Each passage consisted of three independent replicates. B: Immunoblotting of NAMPT protein level in SPGs at different passages. Lower panel shows immunoblotting images. Upper panel shows quantification. C: NAD^+ levels in undifferentiated SPGs at low (P17–P20) and high passages (P56–P59) from three independent replicates. D: Undifferentiated tree shrew SPGs at P53 were treated with different concentrations of NR for one passage. Results showed that 100 μmol/L NR induced the highest level of NAD^+. Data were from three independent replicates. E: Treatment with 100 μmol/L NR for one or three passages using P44 as the testing SPGs significantly increased NAD^+ levels. Data were from three independent replicates. F: Immunoblotting showed that NR treatment in undifferentiated SPGs (P39) over three passages decreased γH2AX levels. Lower panel shows immunoblotting images. Upper panel shows quantification. G: Alkaline comet assay validated the decrease in DNA breaks. At least 200 tails were analyzed in each group across three independent replicates. H–J: NR treatment for three passages at P39 decreased mtDNA copy number (H), cellular ATP concentrations (I), and ROS levels detected by 1 μmol/L DCFH-DA (J). K: Heatmap of DEGs between undifferentiated SPGs treated with or without NR for four passages at P39. Top associated GO terms are shown in right panel. L: mRNA expression levels of several marker genes in tree shrew SSCs were unchanged by NR treatment. Results were based on three independent replicates with similar results. Data are mean±standard deviation (*SD*). ns: Not significant; *: $P<0.05$; **: $P<0.01$; ***: $P<0.001$; two-tailed Student's *t*-test.

induced a gradual increase in NAD^+ (Figure 7E). Intriguingly, treatment for three passages at P39 alleviated DNA damage, as measured by γH2AX immunoblot analysis (Figure 7F; Supplementary Figure S1C) and alkaline comet assay

(Figure 7G). Mitochondrial DNA copy numbers (Figure 7H), ATP production (Figure 7I), and ROS generation (Figure 7J) all decreased after NR treatment for three passages. To better evaluate the effect of NR on undifferentiated SPGs, we performed RNA-seq to compare the gene expression profiles between SPGs (P39) cultured with or without NR for four passages. A total of 65 DEGs were identified, with the majority showing down-regulation in SPGs cultured with NR, suggesting some may be involved in the regulation of metabolism and mitochondrial function (Figure 7K; Supplementary Dataset S2). For instance, *ABCA9* (Piehler et al., 2002; Rath et al., 2021), which plays an important role in metabolism regulation, was significantly down-regulated (Supplementary Figure S2). GO analysis revealed that the NR down-regulated genes were enriched in inflammatory response and complement activation (Figure 7K; Supplementary Dataset S2), consistent with the observation that NR decreased ROS levels and DNA damage, both of which are known to induce inflammation (Kawanishi et al., 2017). However, we did not detect any changes in the expression of marker genes in the undifferentiated SPGs, as validated by further RT-qPCR analysis (Figure 7L). Thus, short-term treatment with NR did not lead to an increase in the SSC population during culture. Future research should explore whether longer treatment durations or the initial inclusion of NR in the culture medium could reduce the depletion of the stem cell pool during prolonged expansion.

DISCUSSION

Tree shrews have emerged as an attractive animal model for a wide range of biomedical research fields including human spermatogenesis (Liu et al., 2023). Various gene-editing techniques, such as SSC-based transgenesis, can be applied in tree shrews (Li et al., 2017). Transplantation of undifferentiated SPGs typically necessitates many cells. For example, approximately 10^5 undifferentiated mouse SPGs are required to restore spermatogenesis in mouse models (Kanatsu-Shinohara et al., 2003), while roughly $2.5x10^7$ SPGs are needed for the restoration of spermatogenesis sufficient to yield detectable spermatozoa in rhesus monkey ejaculate (Hermann et al., 2012). Given these requirements, substantial expansion of undifferentiated tree shrew SPGs is crucial for successful downstream applications. Nevertheless, long-term expansion of stem cells can negatively affect stem cell genetics, epigenetics, and functionality (Helsel et al., 2017; Andrews et al., 2022), the impacts of which need to be clarified. For instance, undifferentiated mouse SPG cultures show a decline in SSC content after 6 months of expansion (Helsel et al., 2017). In this study, we examined the impacts of *ex vivo* expansion of undifferentiated tree shrew SPGs on SSC content and spermatogenesis potential. Our results indicated that undifferentiated tree shrew SPGs cultured for fewer than 30 passages maintained both SSC populations and spermatogenesis potential. However, high-passage (e.g., P55) culture induced SSC population loss and diminished spermatogenesis potential. Concomitant with this decline, we observed marked changes in gene expression between the high-passage (P41 and P53) and low-passage SPGs (<P30). Notably, SPGs at P41 and P53 displayed similar gene expression patterns and were clustered together. Although we did not assess the spermatogenesis potential of SPGs at P41 by transplantation, their gene expression profiles led us to hypothesize that SPGs maintained between passages 40–50 may lose both SSC content and spermatogenesis potential.

During prolonged culture, undifferentiated tree shrew SPGs showed accumulated DNA damage, altered mitochondrial architecture and energy metabolism, and elevated ROS generation. Notably, DEGs up-regulated in high-passage SPGs (>40 passages) were enriched in mitochondrial- and metabolism-related processes, including mitochondrial respiratory chain complex I assembly, ATP production, and ROS generation. Experimental validation confirmed the observed increases in DNA damage, ATP production, and ROS generation, as well as in mitochondrial mass. Mitochondrial complex I is the main generator of ROS in cells. We speculated that authentic SSCs from tree shrews, akin to mouse SSCs (Helsel et al., 2017) and other somatic stem cell types (Rodríguez-Nuevo et al., 2022), may lack a fully assembled complex I in their mitochondria, therefore favoring glycolysis. Previous studies have reported that enhancing glycolytic activity in undifferentiated mouse SPGs supports the long-term maintenance of authentic SSC populations (Helsel et al., 2017). Thus, the metabolism remodeling and concurrent increases in ROS generation and DNA damage may be attributed to loss of SSC content and spermatogenesis potential in long-term cultured tree shrew SPGs. Interestingly, this contrasts sharply with previous research on undifferentiated mouse SPGs, which reported decreased mitochondrial mass and ROS generation and increased glycolysis following 5 years of expanded culture (Kanatsu-Shinohara et al., 2019). These discrepancies may be attributed to difference in culture periods, suggesting that extremely prolonged culture may induce marked metabolism re-wiring.

NAD^+ is a central redox cofactor and the substrate for various enzymes, including SIRTs, PARPs, and cyclic ADP-ribose synthases (Garten et al., 2015). It plays critical roles in regulating mitochondrial function, energy metabolism, DNA damage repair, and many other biological processes (Garten et al., 2015). NAMPT, a rate-limiting enzyme in the NAD^+ salvage pathway (Garten et al., 2015), exhibited significantly down-regulated mRNA and protein expression in high-passage tree shrew SPGs, leading to diminished NAD^+ production in these cells. Given the association between reduced NAD^+ and loss of spermatogenesis potential, we hypothesized that increasing NAD^+ levels in undifferentiated tree shrew SPGs during culture may mitigate metabolic defects and DNA damage, thereby facilitating maintenance of the SSC population after prolonged expansion. Indeed, the addition of the NAD^+ precursor NR to the culture medium for three passages ameliorated deficiencies in mitochondrial function, metabolic activity, and DNA damage. However, short-term NR treatment did not induce substantial changes in gene expression, and notably, did not affect SSC-specific markers. We speculate that short-term treatment (three passages) may be insufficient to improve SSC content and spermatogenesis potential. Future investigations should focus on the beneficial role of NR in long-term expansion of tree shrew SSCs, including its incorporation at the beginning of culture and evaluation through SPG transplantation at varying culture time-points. Taken together, our study sheds light on the impact of long-term expansion on tree shrew SSC properties and proposes a potential strategy for optimizing the culture medium.

DATA AVAILABILITY

RNA-seq data reported in this study were deposited in the Genome Sequence Archive database (http://gsa.big.ac.cn/) under Accession ID (CRA013123), in the Science Data Bank (https://www.scidb.cn/) under DOI: 10.57760/sciencedb.12594, and in the NCBI database under GSE228744.

SUPPLEMENTARY DATA

Supplementary data to this article can be found online.

COMPETING INTERESTS

The authors declare that they have no competing interests.

AUTHORS' CONTRIBUTIONS

C.L. performed most of the experiments and wrote the draft. R.B. and C.L. performed the transplantation assays. L.W. analyzed the RNA-seq data. Y.H.M. cared for the tree shrews. P.Z. and Y.G.Y. designed and supervised the study and revised the manuscript. All authors read and approved the final version of the manuscript.

REFERENCES

Andrews PW, Barbaric I, Benvenisty N, et al. 2022. The consequences of recurrent genetic and epigenetic variants in human pluripotent stem cells. *Cell Stem Cell*, **29**(12): 1624−1636.

Bi R, Li C, Ma YH, et al. 2021a. Depletion of endogenous germ cells of tree shrew. *In*: Embryo Manipulation Manual of Laboratory Animals. *Bio-101*, doi:https://doi.org/10.21769/BioProtoc.10101933. (in Chinese)

Bi R, Li C, Zheng QZ, et al. 2021b. Transplantation of spermatogenic stem cells of tree shrew. *In*: Embryo Manipulation Manual of Laboratory Animals. *Bio-101*, doi:https://doi.org/10.21769/BioProtoc.1010936. (in Chinese)

Bi R, Li Y, Xu M, et al. 2022. Direct evidence of CRISPR-Cas9-mediated mitochondrial genome editing. *The Innovation*, **3**(6): 100329.

Bieganowski P, Brenner C. 2004. Discoveries of nicotinamide riboside as a nutrient and conserved *NRK* genes establish a Preiss-Handler independent route to NAD^+ in fungi and humans. *Cell*, **117**(4): 495−502.

Brinster RL, Zimmermann JW. 1994. Spermatogenesis following male germ-cell transplantation. *Proceedings of the National Academy of Sciences of the United States of America*, **91**(24): 11298−11302.

Chen W, Zhang ZR, Chang C, et al. 2020. A bioenergetic shift is required for spermatogonial differentiation. *Cell Discovery*, **6**(1): 56.

Chen Y, Zheng YX, Gao Y, et al. 2018. Single-cell RNA-seq uncovers dynamic processes and critical regulators in mouse spermatogenesis. *Cell Research*, **28**(9): 879−896.

Familtsev D, Quiggins R, Masterson SP, et al. 2016. Ultrastructure of geniculocortical synaptic connections in the tree shrew striate cortex. *Journal of Comparative Neurology*, **524**(6): 1292−1306.

Fan Y, Huang ZY, Cao CC, et al. 2013. Genome of the Chinese tree shrew. *Nature Communications*, **4**: 1426.

Fan Y, Ye MS, Zhang JY, et al. 2019. Chromosomal level assembly and population sequencing of the Chinese tree shrew genome. *Zoological Research*, **40**(6): 506−521.

Garten A, Schuster S, Penke M, et al. 2015. Physiological and pathophysiological roles of NAMPT and NAD metabolism. *Nature Reviews Endocrinology*, **11**(9): 535−546.

Guo JT, Grow EJ, Mlcochova H, et al. 2018. The adult human testis transcriptional cell atlas. *Cell Research*, **28**(12): 1141−1157.

Han XP, Wang RY, Zhou YC, et al. 2018. Mapping the mouse cell atlas by microwell-seq. *Cell*, **173**(5): 1307.

Helsel AR, Oatley MJ, Oatley JM. 2017. Glycolysis-optimized conditions enhance maintenance of regenerative integrity in mouse spermatogonial stem cells during long-term culture. *Stem Cell Reports*, **8**(5): 1430−1441.

Hermann BP, Sukhwani M, Winkler F, et al. 2012. Spermatogonial stem cell transplantation into rhesus testes regenerates spermatogenesis producing functional sperm. *Cell Stem Cell*, **11**(5): 715−726.

Izadyar F, Spierenberg GT, Creemers LB, et al. 2002. Isolation and purification of type A spermatogonia from the bovine testis. *Reproduction*, **124**(1): 85−94.

Kanatsu-Shinohara M, Inoue K, Ogonuki N, et al. 2011. Serum- and feeder-free culture of mouse germline stem cells. *Biology of Reproduction*, **84**(1): 97−105.

Kanatsu-Shinohara M, Ogonuki N, Inoue K, et al. 2003. Long-term proliferation in culture and germline transmission of mouse male germline stem cells. *Biology of Reproduction*, **69**(2): 612−616.

Kanatsu-Shinohara M, Shinohara T. 2013. Spermatogonial stem cell self-renewal and development. *Annual Review of Cell and Developmental Biology*, **29**: 163−187.

Kanatsu-Shinohara M, Yamamoto T, Toh H, et al. 2019. Aging of spermatogonial stem cells by Jnk-mediated glycolysis activation. *Proceedings of the National Academy of Sciences of the United States of America*, **116**(33): 16404−16409.

Kawanishi S, Ohnishi S, Ma N, et al. 2017. Crosstalk between DNA damage and inflammation in the multiple steps of carcinogenesis. *International Journal of Molecular Sciences*, **18**(8): 1808.

Kubota H, Avarbock MR, Brinster RL. 2004. Growth factors essential for self-renewal and expansion of mouse spermatogonial stem cells. *Proceedings of the National Academy of Sciences of the United States of America*, **101**(47): 16489−16494.

Kubota H, Brinster RL. 2018. Spermatogonial stem cells. *Biology of Reproduction*, **99**(1): 52−74.

Lau LMS, Dagg RA, Henson JD, et al. 2013. Detection of alternative lengthening of telomeres by telomere quantitative PCR. *Nucleic Acids Research*, **41**(2): e34.

Lee KS, Huang XY, Fitzpatrick D. 2016. Topology of ON and OFF inputs in visual cortex enables an invariant columnar architecture. *Nature*, **533**(7601): 90−94.

Li C, Bi R, Zheng P. 2021. Establishment of spermatogenic stem cell lines from tree shrew. *In*: Embryo Manipulation Manual of Laboratory Animals. *Bio-101*, doi:https://doi.org/10.21769/BioProtoc.1010935. (in Chinese)

Li CH, Yan LZ, Ban WZ, et al. 2017. Long-term propagation of tree shrew spermatogonial stem cells in culture and successful generation of transgenic offspring. *Cell Research*, **27**(2): 241−252.

Liu CY, Si W, Tu CF, et al. 2023. Deficiency of primate-specific *SSX1* induced asthenoteratozoospermia in infertile men and cynomolgus monkey and tree shrew models. *American Journal of Human Genetics*, **110**(3): 516−530.

Lord T, Nixon B. 2020. Metabolic changes accompanying spermatogonial stem cell differentiation. *Developmental Cell*, **52**(4): 399−411.

Mouchiroud L, Houtkooper RH, Moullan N, et al. 2013. The NAD^+/Sirtuin pathway modulates longevity through activation of mitochondrial UPR and FOXO signaling. *Cell*, **154**(2): 430−441.

Nagano M, Avarbock MR, Leonida EB, et al. 1998. Culture of mouse spermatogonial stem cells. *Tissue and Cell*, **30**(4): 389−397.

Oancea M, Mazumder S, Crosby ME, et al. 2006. Apoptosis assays. *Methods in Molecular Medicine*, **129**: 279−290.

Piehler A, Kaminski WE, Wenzel JJ, et al. 2002. Molecular structure of a novel cholesterol-responsive A subclass ABC transporter, ABCA9. *Biochemical and Biophysical Research Communications*, **295**(2): 408−416.

Rath S, Sharma R, Gupta R, et al. 2021. MitoCarta3.0: an updated mitochondrial proteome now with sub-organelle localization and pathway annotations. *Nucleic Acids Research*, **49**(D1): D1541−D1547.

Rodríguez-Nuevo A, Torres-Sanchez A, Duran JM, et al. 2022. Oocytes maintain ROS-free mitochondrial metabolism by suppressing complex I. *Nature*, **607**(7920): 756−761.

Rogakou EP, Pilch DR, Orr AH, et al. 1998. DNA double-stranded breaks induce histone H2AX phosphorylation on serine 139. *Journal of Biological*

Chemistry, **273**(10): 5858−5868.
Rubin H. 2002. The disparity between human cell senescence *in vitro* and lifelong replication *in vivo*. *Nature Biotechnology*, **20**(7): 675–681.
Ryall JG, Cliff T, Dalton S, et al. 2015. Metabolic reprogramming of stem cell epigenetics. *Cell Stem Cell*, **17**(6): 651−662.
Savier E, Sedigh-Sarvestani M, Wimmer R, et al. 2021. A bright future for the tree shrew in neuroscience research: summary from the inaugural Tree Shrew Users Meeting. *Zoological Research*, **42**(4): 478−481.
Schmidt JA, Abramowitz LK, Kubota H, et al. 2011. In vivo and in vitro aging is detrimental to mouse spermatogonial stem cell function. *Biology of Reproduction*, **84**(4): 698−706.
Shami AN, Zheng XN, Munyoki SK, et al. 2020. Single-cell RNA sequencing of human, macaque, and mouse testes uncovers conserved and divergent features of mammalian spermatogenesis. *Developmental Cell*, **54**(4): 529−547.e12.
Sun YZ, Liu ST, Li XM, et al. 2019. Progress in *in vitro* culture and gene editing of porcine spermatogonial stem cells. *Zoological Research*, **40**(5): 343−348.
Swain U, Rao KS. 2011. Study of DNA damage via the comet assay and base excision repair activities in rat brain neurons and astrocytes during aging. *Mechanisms of Ageing and Development*, **132**(8-9): 374−381.
Trapnell C, Hendrickson DG, Sauvageau M, et al. 2013. Differential analysis of gene regulation at transcript resolution with RNA-seq. *Nature Biotechnology*, **31**(1): 46−53.
Trapnell C, Roberts A, Goff L, et al. 2012. Differential gene and transcript expression analysis of RNA-seq experiments with TopHat and Cufflinks. *Nature Protocols*, **7**(3): 562−578.
Veit J, Bhattacharyya A, Kretz R, et al. 2011. Neural response dynamics of spiking and local field potential activity depend on CRT monitor refresh rate in the tree shrew primary visual cortex. *Journal of Neurophysiology*, **106**(5): 2303−2313.
Voigt AL, Thiageswaran S, de Lima e Martins Lara N, et al. 2021. Metabolic requirements for spermatogonial stem cell establishment and maintenance in vivo and in vitro. *International Journal of Molecular Sciences*, **22**(4): 1998.
Wang XL, Yin LS, Wen YJ, et al. 2022. Mitochondrial regulation during male germ cell development. *Cellular and Molecular Life Sciences*, **79**(2): 91.
Wu J, Ocampo A, Belmonte JCI. 2016. Cellular metabolism and induced pluripotency. *Cell*, **166**(6): 1371−1385.
Xiao J, Liu R, Chen CS. 2017. Tree shrew (*Tupaia belangeri*) as a novel laboratory disease animal model. *Zoological Research*, **38**(3): 127−137.
Xu L, Chen SY, Nie WH, et al. 2012. Evaluating the phylogenetic position of chinese tree shrew (*Tupaia belangeri chinensis*) based on complete mitochondrial genome: implication for using tree shrew as an alternative experimental animal to primates in biomedical research. *Journal of Genetics and Genomics*, **39**(3): 131−137.
Xu L, Yu D, Yao YL, et al. 2020a. Tupaia MAVS is a dual target during hepatitis C virus infection for innate immune evasion and viral replication via NF-κB. *Journal of Immunology*, **205**(8): 2091−2099.
Xu L, Yu DD, Ma YH, et al. 2020b. COVID-19-like symptoms observed in Chinese tree shrews infected with SARS-CoV-2. *Zoological Research*, **41**(5): 517−526.
Yamanaka S. 2020. Pluripotent stem cell-based cell therapy—promise and challenges. *Cell Stem Cell*, **27**(4): 523−531.
Yang JH, Hayano M, Griffin PT, et al. 2023. Loss of epigenetic information as a cause of mammalian aging. *Cell*, **186**(2): 305−326.e27.
Yao YG. 2017. Creating animal models, why not use the Chinese tree shrew (*Tupaia belangeri chinensis*)?. *Zoological Research*, **38**(3): 118−126.
Ye MS, Zhang JY, Yu DD, et al. 2021. Comprehensive annotation of the Chinese tree shrew genome by large-scale RNA sequencing and long-read isoform sequencing. *Zoological Research*, **42**(6): 692−709.
Yu WH, Yang CC, Bi YH, et al. 2016. Characterization of hepatitis E virus infection in tree shrew (*Tupaia belangeri chinensis*). *BMC Infectious Diseases*, **16**: 80.
Zapata-Pérez R, Wanders RJA, van Karnebeek CDM, et al. 2021. NAD^+ homeostasis in human health and disease. *EMBO Molecular Medicine*, **13**(7): e13943.
Zhan LJ, Ding HR, Lin SZ, et al. 2014. Experimental *Mycobacterium tuberculosis* infection in the Chinese tree shrew. *FEMS Microbiology Letters*, **360**(1): 23−32.
Zhang WD, Tang M, Wang L, et al. 2023. *Lnc956*-TRIM28-HSP90B1 complex on replication forks promotes CMG helicase retention to ensure stem cell genomic stability and embryogenesis. *Science Advances*, **9**(4): eadf6277.
Zhao B, Zhang WD, Cun YX, et al. 2018. Mouse embryonic stem cells have increased capacity for replication fork restart driven by the specific Filia-Floped protein complex. *Cell Research*, **28**(1): 69−89.
Zhao B, Zhang WD, Duan YL, et al. 2015. Filia is an ESC-specific regulator of DNA damage response and safeguards genomic stability. *Cell Stem Cell*, **16**(6): 684−698.
Zheng P. 2022. Current understanding of genomic stability maintenancein pluripotent stem cells. *Acta Biochimica et Biophysica Sinica*, **54**(6): 858−863.
Zheng Y, Feng TY, Zhang PF, et al. 2020. Establishment of cell lines with porcine spermatogonial stem cell properties. *Journal of Animal Science and Biotechnology*, **11**: 33.
Zheng Y, Jongejan A, Mulder CL, et al. 2017. Trivial role for NSMCE2 during *in vitro* proliferation and differentiation of male germline stem cells. *Reproduction*, **154**(3): 181−195.